Article

Not peer-reviewed version

Combining Silica-Loaded Iron-Catalyzed Sodium Percarbonate (SPC^{SF}) with *Bacillus subtilis* for Enhanced Remediation of Diesel-Contaminated Soil: Performance and Synergistic Mechanisms

Beibei Ren , Wei Wei * , Mingli Wei , Siguang Zhao *

Posted Date: 27 February 2026

doi: 10.20944/preprints202602.1798.v1

Keywords: sodium percarbonate; Fenton-like oxidation; *Bacillus subtilis*; petroleum hydrocarbon; soil remediation; synergistic mechanism

 doi:10.20944/preprints202602.1798.v1

Article

Combining Silica-Loaded Iron-Catalyzed Sodium Percarbonate (SPC^{SF}) with *Bacillus subtilis* for Enhanced Remediation of Diesel-Contaminated Soil: Performance and Synergistic Mechanisms

Beibei Ren [1,2,3], Wei Wei [4,*], Mingli Wei [4,5] and Siguang Zhao [1,3,*]

[1] State Key Laboratory of Intelligent Construction and Healthy Operation and Maintenance of Deep Underground Engineering, China University of Mining and Technology, Xuzhou, Jiangsu 221116, China
[2] Jiangsu Vocational Institute of Architectural Technology, Xu Zhou, Jiang Su 221116, China
[3] School of Mechanics and Civil Engineering, China University of Mining and Technology, Xuzhou, Jiangsu 221116, China
[4] State Key Laboratory of Geomechanics and Geotechnical Engineering, Institute of Rock and Soil Mechanics, Chinese Academy of Sciences, Wuhan, 430071, China
[5] Jiangsu Institute of Zoneco Co., Ltd., Yixing, 214200, China
* Correspondence: weiwei204@mails.ucas.ac.cn; zhaoguangsi@cumt.edu.cn

Abstract

Petroleum hydrocarbon contamination in soil is difficult to remediate due to strong adsorption and limited bioavailability. In this study, a combined remediation strategy integrating a silica gel-loaded, iron-catalyzed sodium percarbonate composite (SPCSF) with Bacillus subtilis ATCC 11774 was developed for diesel-contaminated soil. The remediation performance of chemical oxidation, microbial remediation, and their combined application was systematically evaluated. The simultaneous SPCSF–microbial treatment achieved the highest removal efficiency, reaching 65.1% after 31 d, which was markedly higher than that of chemical oxidation (22.5%) or microbial remediation alone (31.1%). SPCSF played a dual role in the system: it generated reactive oxygen species for the oxidative breakdown of long-chain hydrocarbons into bioavailable intermediates, and it regulated soil pH and oxidation–reduction potential, creating favorable conditions for microbial activity. In turn, Bacillus subtilis facilitated Fe(II) reduction and stabilization, sustaining the Fe(II)/Fe(III) redox cycle and thereby enhancing hydroxyl radical generation in Fenton-like reactions. Spectroscopic analyses (three-dimensional fluorescence spectrum, Fourier transform infrared spectroscopy, and X-ray photoelectron spectroscopy) demonstrated that the combined treatment promoted the transformation of petroleum hydrocarbons into carboxyl-rich organic matter, providing molecular-scale evidence of effective mineralization. This synergistic interaction between chemical oxidation and microbial degradation offers an efficient and environmentally compatible approach for petroleum hydrocarbon–contaminated soil remediation.

Keywords: sodium percarbonate; Fenton-like oxidation; Bacillus subtilis; petroleum hydrocarbon; soil remediation; synergistic mechanism

1. Introduction

Petroleum hydrocarbons, as essential resources for industrialization, have been extensively exploited worldwide [1, 2]. Increasing demand has driven the construction of numerous petroleum extraction and storage facilities (e.g., oil wells, and storage tanks), including oil wells and storage tanks, which has consequently has led to frequent leakage events and transportation accidents [3, 4]. These incidents cause severe ecological damage, manifested by soil fertility degradation and alterations in soil physicochemical properties. As a result, petroleum pollution has emerged as a

 doi:10.20944/preprints202602.1798.v1

global environmental concern [5]. Current remediation technologies are generally classified into physical, chemical, and biological approaches [6-9]. Among them, microbial remediation has attracted considerable attention because it produces no secondary pollution, is cost-effective, and exhibits strong sustainability [7]. However, its effectiveness is often limited in degrading structurally complex petroleum hydrocarbons that are strongly adsorbed onto soil particle surfaces. Moreover, remediation performance is highly sensitive to environmental conditions such as temperature and soil pH [10, 11], and the process typically requires long treatment periods, resulting in substantial time costs.

To address these limitations, chemical oxidation have recently integrated with microbial remediation [8, 12]. Chemical oxidation can rapidly degrade recalcitrant compounds; however, it generally requires large quantities of oxidants. Excessive oxidant dosages have been reported to adversely affect soil properties, including pH and organic matter content, thereby impairing the soil environment [13]. By contrast, the combined strategy mitigates the low efficiency of microbial remediation and reduces the high oxidant demand and associated environmental risks of chemical oxidant, making it a promising approach for soil remediation.

Despite these advantages, many commonly used oxidants exhibit pronounced microbial toxicity, which restricts their applicability in combined remediation systems [14, 15]. For instance, sodium persulfate generates $SO_4^{\cdot-}$ radicals that can inhibit or inactivate microorganisms [16, 17]. Although the Fenton reagent is less toxic than persulfate, high concentrations still significantly suppress microbial activity [18]. Even though microbial communities may partially recover after treatment, excessive oxidant exposure can induce irreversible changes in community structure and genetic composition [19]. In addition, the short half-life of H_2O_2 (from minutes to hours) poses a further challenge. Nonuniform distribution in soil can create localized regions with high H_2O_2 concentrations, which promotes direct decomposition into H_2O and O_2 rather than participation in Fenton reactions [20]. This competing pathway dominates H_2O_2 consumption and markedly reduces oxidation efficiency.

Sodium percarbonate (SPC) has recently been recognized as a promising oxidant for organic contamination remediation [21, 22]. As an H_2O_2-Na_2CO_3 adduct, SPC decomposes in aqueous environments to release H_2O_2, Na^+, and CO_3^{2-}, thereby enabling pollutant degradation through Fenton reactions. In comparison with direct H_2O_2 application, SPC offers improved handling safety, enhanced transportation security, and broader pH adaptability. Its slow-release behavior effectively prevents localized accumulation of H_2O_2, which reduces microbial toxicity and undesired side reactions while improving H_2O_2 utilization efficiency. Furthermore, Pan, et al. [23] demonstrated that SPC addition can stimulate microbial metabolic activity in contaminated sediments by supplying electron acceptors or donors, highlighting its potential as a cost-effective ecological engineering strategy. In previous work, we further improved component stability and remediation efficiency by developing silica-based carriers for SPC and $FeSO_4$ in Fenton systems.

In this study, *Bacillus subtilis* was combined with a silica gel-loaded, iron-catalyzed SPC composite (SPC^{SF}) for the remediation of petroleum hydrocarbon-contaminated soil. The remediation performance of SPC^{SF} alone, microbial treatment alone, and their combination application, including simultaneous and sequential modes, was systematically compared, and the influence of SPC^{SF} on microbial growth was evaluated. The objectives of this work were to determine the optimal bacterial inoculum size under combined treatment conditions, to assess the effects of microbial activity on soil physicochemical properties (pH, oxidation-reduction potential), and to elucidate the remediation mechanisms of the SPC^{SF}-bacteria system for petroleum hydrocarbon-contaminated soil using X-ray photoelectron spectroscopy (XPS), Fourier transform infrared spectroscopy (FTIR), and three-dimensional fluorescence spectrum (3D-EEM.) The results provide mechanistic insights and performance evaluation for SPC-microbial combined remediation, thereby supporting its engineering application in petroleum hydrocarbon-contaminated soils.

2. Materials and Methods

2.1. Soil and Reagent

 doi:10.20944/preprints202602.1798.v1

The test soil used in this study was commercial kaolin. As one of the fundamental clay minerals widely present in natural soils, kaolinite is commonly used as a model soil in laboratory experiments. In addition, commercial kaolin contains a low organic matter content, which helps to minimize interference from background organic substances with reaction processes. Commercial 0# diesel, a representative petroleum hydrocarbon, was selected as the target contaminant. The physicochemical properties of the kaolin and 0# diesel are presented in Table 1.

Chemical oxidation was conducted using supported sodium percarbonate as the oxidizing agent and supported ferrous sulfate as the catalytic material. The composition of the supported sodium percarbonate and supported ferrous sulfate are summarized in Fig.1a.

The petroleum hydrocarbon-degrading bacterium used in this study was *Bacillus subtilis* ATCC 11774, which has been reported to exhibit effective hydrocarbon degradation capability. The strain was purchased from China Biosep Group Co., Ltd.

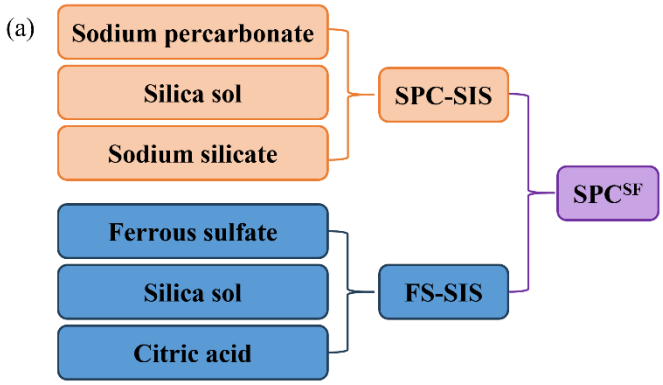

(b)

	SPC^{SF}	Bacteria solution
S	√	×
B	×	√
BS	√ ①	√ ①
SB	√ ①	√ ②

Figure 1. Schematic diagram of SPC^{SF} preparation and experimental design. In Fig. 1a, SPC-SIS was used as the oxidizing agent and FS-SIS was used as the catalyst. In Fig. 1b, "√" indicates that the corresponding remediation approach was applied, whereas "×" indicates that it was not applied. Symbols ① and ② denote the sequence of remediation application.

2.2. Artificial Contamination

The kaolin was passed through a 2 mm sieve, and the soil samples were oven-dried at 105°C for 24 h, followed by cooling to room temperature and sealed storage. Diesel was uniformly sprayed onto the surface of the kaolin and thoroughly mixed for 5 min to ensure homogeneous contaminant distribution. The contaminated soil was then aged at 4°C for 7 days. The initial petroleum hydrocarbon concentration in the kaolin was 10229.640 mg/kg.

2.3. Preparation of Oxidizing Agents and Microbial Cultivation

The preparation procedure of the chemical oxidation agents followed a previously reported method [1]. The purchased bacterial strain was first inoculated onto solid Luria-Bertani (LB) medium plates and incubated in a biochemical incubator at 25°C for 1 day to achieve activation. The LB liquid medium consisted of tryptone (10 g/L), yeast extract (5 g/L), and sodium chloride (10 g/L), while the LB solid medium was prepared by adding 20 g/L agar to the liquid medium formulation. After activation, the strain was transferred into LB liquid medium and cultivated for 2 days to obtain a bacterial suspension. The optical density of the suspensions was measured at a wavelength of 600 nm (OD600) using a spectrophotometer (UV-1800, Shimadzu, Japan), and OD_{600} values were used to represent bacterial concentration. When OD_{600} values ranged from 0.2 and 0.8, the following conversion relationship was applied:

$$Y=8.59\times10^{7}\times OD_{600}^{1.3627} \quad (1)$$

This section may be divided by subheadings. It should provide a concise and precise description of the experimental results, their interpretation, as well as the experimental conclusions that can be drawn.

2.4. Degradation of Pollutant

 doi:10.20944/preprints202602.1798.v1

Pollutant degradation experiments were conducted using four treatment groups: chemical oxidation, the microbial remediation, pre-oxidation combined with microbial remediation, and oxidation combined with microbial remediation. Detailed information is shown in Fig. 1b. In the chemical oxidation and microbial remediation groups, contaminated soil was treated exclusively with chemical reagents or microorganisms, respectively. In the pre-oxidation combined with microbial remediation group, the contaminated soil was first subjected to chemical oxidation for 10 days, after which a bacterial suspension was introduced for subsequent microbial remediation. In the oxidation combined with microbial remediation group, oxidants and bacterial suspension were simultaneously added to the soil to achieve pollutant removal.

In all treatments involving chemical oxidation, SPC^{SF} was applied at a dosage of 1% of the dry soil weight, while the bacterial suspension was added at levels specified in Table 2. Soil samples from each treatment group were collected on days 5, 10, 17, 24, and 31 days for subsequent analyses.

2.5. Analysis Method

Changes in physicochemical properties during the remediation process, which serve as key indicators of remediation progress, were measured and evaluated. Oxidation-reduction potential (ORP) and pH were determined using an InLab Redox Electrode and an InLab Routine Pro electrode connected to an FE-28 meter. For these measurements, a soil-to-water ratio of 1:2.5 was maintained.

The abundance of petroleum hydrocarbon-degrading bacteria in soil was quantified using the plate dilution counting method. Briefly, 1 g of soil sample was transferred into a conical flask containing 99 mL of sterile water and thoroughly homogenized. Serial dilutions were then prepared to obtain microbial suspensions at dilution levels of 10^{-3}, 10^{-4}, 10^{-5}, and 10^{-6} relative to the original sample. Subsequently, 0.1 mL aliquots of each dilution were spread onto LB solid medium plates. The plates were incubated at 25°C in a constant-temperature biochemical incubator for 24 h, after which colony numbers were counted.

To investigate carbon transformation in contaminated soil during chemical oxidation and biodegradation processes, dissolved organic matter (DOM) in the samples was characterized using 3D-EEM. For sample preparation, 5 g of soil was weighed and transferred into a 50 mL centrifuge tube, after which deionized water was added at a soil-to-water ratio of 5:1. The tube was placed in a constant-temperature shaker and agitated at 25°C and 170 rpm for 24 hours. After agitation, the suspension was centrifuged at 3000 rpm for 10 min. The supernatant was then collected and passed through a 0.45 μm membrane filter. The filtrate was stored at 4°C prior to 3D-EEM analysis.

3D-EEM measurements were performed using a Hitachi F-4600 fluorescence spectrophotometer equipped with a 150 W xenon arc lamp. The excitation wavelength (Ex) was scanned from 200 to 400 nm, and the emission wavelength (Em) was scanned from 250 nm to 550 nm. The wavelength increments were set at 5 nm for excitation and 2 nm for emission, with a scan speed of 1200 nm/min. The obtained fluorescence data were processed using MATLAB R2012a to remove Raman and Rayleigh scattering effects.

The physicochemical properties of samples were characterized using XPS and FTIR. The chemical states of surface elements, including C and Fe, were determined using a K-Alpha XPS system (Escalab 250Xi, Thermo Fisher, USA). The analysis was conducted with a spot diameter of 500 μm, a pass energy of 30 eV, and a step size of 0.1 eV. All spectra were calibrated by referencing the C 1s peak to a binding energy of 284.8 eV in order to correct for charging effects. Peak fitting of the XPS spectra was performed using Avantage software.

Fourier transform infrared spectroscopy was carried out using a Nicolet 380 spectrometer (Thermo Fisher Scientific, USA) to characterize surface functional groups in the soil samples. The soil was passed through a 0.075 mm sieve, and the obtained powder was homogenized with potassium bromide (KBr) to prepare pellets for analysis. Spectra were collected at a resolution of 4 cm^{-1} over a wavenumber range of 400–4000 cm^{-1}.

3. Materials and Methods

3.1. Performance of Pollutant Removal

 doi:10.20944/preprints202602.1798.v1

Figure 2 presents the removal efficiencies of different treatment groups. The simultaneous application of chemical oxidation and microbial remediation exhibited the highest removal performance among all treatments, with the B40RS1 group achieving a final removal efficiency of 65.1%. In contrast, chemical oxidation alone resulted in a removal efficiency of only 22.5% at 31 d, which was lower than that observed for all other treatment groups.

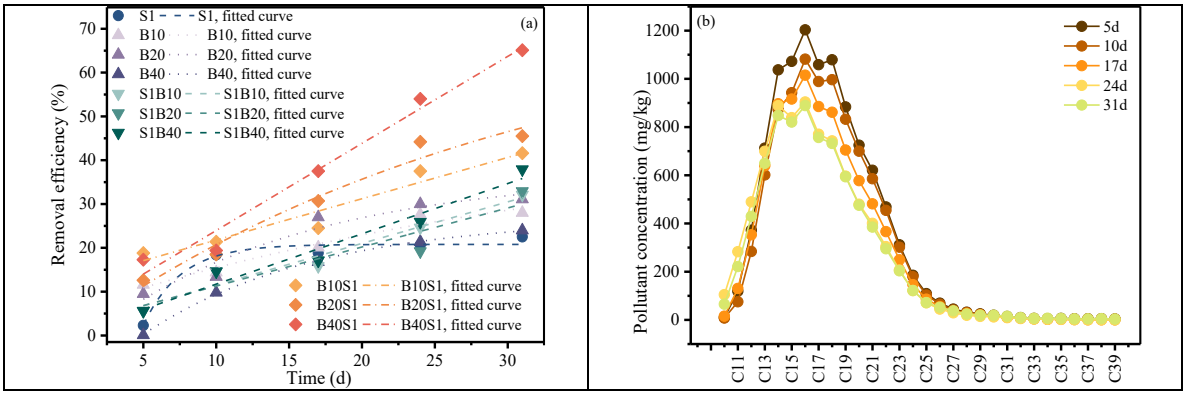

Figure 2. Diesel removal efficiency of different treatment groups (a) and concentrations of diesel hydrocarbons with different carbon chain lengths (C10–C40) (b). In the group notation, the number "1" in S1 denotes that the dosage of the chemical oxidant was 1% of the dry soil weight; the number "10" in B10 indicates the volume of bacterial suspension added. In S1B10, "1" represents a chemical oxidant dosage of 1% of the dry soil weight, and "10" represents the volume of bacterial suspension added. The numerical designations in other groups follow the same convention.

The microbial remediation group and the pre-oxidation combined with microbial remediation group showed generally comparable overall diesel removal efficiencies. In the microbial-only treatment, the removal efficiency initially increased and subsequently decreased with increasing bacterial suspension volume. The maximum removal efficiency in this group was 31.1% at 31 d with a bacterial suspension volume of 20 mL. In contrast, following pre-oxidation, diesel degradation increased consistently with increasing bacterial suspension volume, reaching a final removal efficiency of 37.9%.

In the microbial-only group, limited nutrient availability induced competition among microorganisms, which constrained metabolic activity and resulted in relatively lower removal efficiency. After pre-oxidation, alkane compounds were transformed into smaller carbon molecules that served as accessible nutrients for Bacillus subtilis. As a result, the difference in removal efficiency between the microbial-only and pre-oxidation groups gradually decreased after the bacterial suspension was introduced on day 10. By day 31, the pre-oxidation combined with microbial remediation group consistently exhibited higher removal efficiency than the microbial-only group.

Chemical oxidation was conducted using supported sodium percarbonate as the oxidizing agent and supported ferrous sulfate as the catalytic material. The composition of the supported sodium percarbonate and supported ferrous sulfate are summarized in Fig.1a.

The petroleum hydrocarbon-degrading bacterium used in this study was *Bacillus subtilis* ATCC 11774, which has been reported to exhibit effective hydrocarbon degradation capability. The strain was purchased from China Biosep Group Co., Ltd.

3.2. Physicochemical Environment Regulation

3.2.1. pH

Soil pH plays a critical role in regulating microbial growth and activity during the remediation process. As shown in Fig. 3a, the pH of the virgin soil was approximately 9.70, indicating strong alkalinity that is unfavorable for microbial survival. Compared with the blank group, the pH of the SPC^{SF}-amended group (S1) was reduced. This decrease was primarily attributed to the acidifying effect of citric acid present in SPC^{SF}, which effectively lowered soil alkalinity and thereby created more favorable conditions for microbial growth. In group S1, a gradual increase in pH with curing

 doi:10.20944/preprints202602.1798.v1

time was observed, which can be ascribed to the neutralization effect of alkaline sodium carbonate generated during the decomposition of sodium percarbonate.

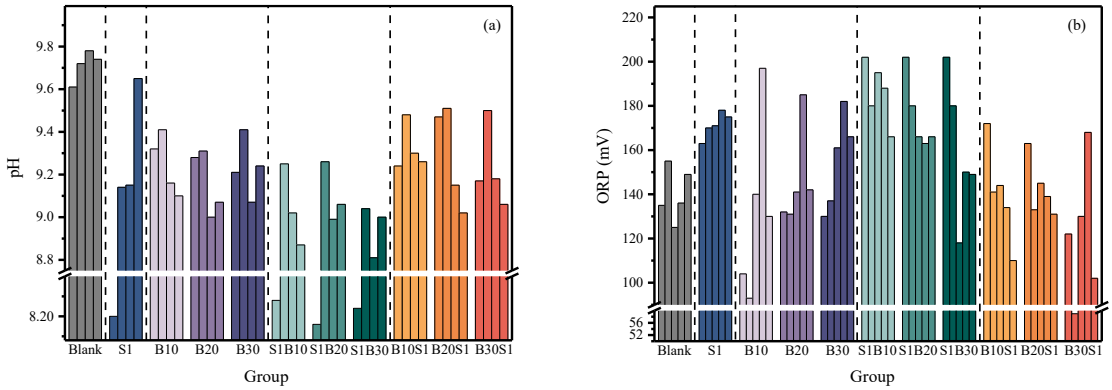

Figure 3. Changes in soil physicochemical properties during remediation: (a) pH, (b) oxidation–reduction potential (ORP). In the group notation, the number "1" in S1 denotes that the dosage of the chemical oxidant was 1% of the dry soil weight; the number "10" in B10 indicates the volume of bacterial suspension added. In S1B10, "1" represents a chemical oxidant dosage of 1% of the dry soil weight, and "10" represents the volume of bacterial suspension added. The numerical designations in other groups follow the same convention.

During microbial remediation, microorganisms catabolized amino acids from the LB medium to sustain metabolic activity and meet nutrient demands. This process was accompanied by the release of NH_4^+, resulting in an increase in soil pH. As nutrients in the LB medium were progressively depleted, microorganisms shifted their metabolic pathways to utilize pollutants as carbon sources. The subsequent degradation of these pollutants led to the production of organic acids and the release of H^+, ultimately causing a decrease in soil pH.

Similarly, in the SB groups with delayed bacterial inoculation, pH values increased following the addition of the bacterial suspension on day 10. This initial increase can be attributed to the continued accumulation of carbonate derived from sodium percarbonate decomposition. Subsequently, as microbial metabolic activity intensified, the generation of organic acids resulted in a gradual decline in soil pH. Accordingly, higher bacterial inoculation levels led to a more pronounced reduction in pH.

The combined remediation groups (BS) exhibited a pH variation pattern similar to that observed in the SB group. On day 10, the pH values of groups S1B1, S1B2, and S1B3 were 9.24, 9.47, and 9.17, respectively, which were higher than that of group S1 (8.42). This difference can be attributed to microbial activity that likely consumed citric acid derived from SPC^{SF}, thereby weakening its acidifying effect and resulting in relatively higher pH values during the early stage of remediation.

3.2.2. ORP

Oxidation-redox potential (ORP) reflects the macroscopic oxidation redox conditions within soil systems. As shown in Fig. 3b, compared with the blank control group, the S1 group exhibited consistently higher ORP from 5 d to 31 d. This increase was mainly attributed to the addition of SPCSF, which generated strong oxidizing species, such as hydroxyl radicals (OH·), thereby creating an oxidative environment in the soil and promoting the degradation of petroleum hydrocarbon contaminants.

In the B groups, the ORP values of groups B1, B2, and B3 showed a slow overall increase during the 31 d remediation period. During the first 10 d, the ORP value were slightly lower than those of the blank control group and then gradually declined. During the remediation of petroleum hydrocarbon-contaminated soil by Bacillus subtilis, aerobic respiration represents the dominant metabolic pathway. In this process, petroleum hydrocarbons, serving as both carbon and energy sources, are progressively oxidized and decomposed. The electrons (e-) and protons (H+) generated are transferred through a series of electron carriers, such as NADH, $FADH_2$, to the terminal electron acceptor, oxygen (O_2), resulting in the formation of water (H_2O). This respiratory activity leads to the

 doi:10.20944/preprints202602.1798.v1

accumulation of reduced coenzymes and electron carriers, thereby causing a gradual decrease in redox potential with increasing remediation time and microbial abundance.

During the pre-oxidation stage, sodium percarbonate oxidized petroleum hydrocarbon contaminants into small-molecular carbon compounds, which subsequently served as carbon sources for microbial metabolism and facilitated the formation of reduced coenzymes. Consequently, the overall decline in ORP was more pronounced than that observed in the B groups. In the BS groups, sodium percarbonate dominated the initial remediation stage. As the oxidizing agent was gradually consumed, microorganisms increasingly contributed to pollutant degradation. As a result, ORP values remained relatively high at the early stage and then gradually decreased throughout the remediation period.

3.3. Mechanism of Enhanced Remediation

To elucidate the synergistic mechanism responsible for the enhanced remediation performance of the SPC^{SF}–microbial system, the transformation of organic carbon, regulation of soil redox conditions, and iron speciation were systematically investigated using spectroscopic and electrochemical techniques.

3.3.1. Transformation of Petroleum Hydrocarbons and DOM Evolution

Changes in soil organic matter composition reflect both the transformation of petroleum hydrocarbons and the growth and metabolic activity of microorganisms. 3D-EEM was employed to characterize the composition and evolution of dissolved organic matter. As shown in Fig. 4a-4b, the fluorescence signals were classified into five regions: I (aromatic protein I), II (aromatic protein II), III (fulvic-like acids), IV (soluble microbial byproducts), and V (humic-like acids). Fig. 4a presents the 3D-EEM spectra of the original contaminated soil, in which region II dominated the fluorescence response. After remediation, additional fluorescence signals appeared in regions III, IV, and V, indicating the formation of fulvic-like and protein-like substances. These components were generated through the cleavage of C–C and C–H bonds in long-chain diesel hydrocarbons under the combined action of SPC^{SF} and microorganisms, producing low-molecular-weight aliphatic intermediates. These intermediates were subsequently assimilated by microorganisms for biomass synthesis and organic matter production, thereby enhancing DOM abundance and fluorescence intensities in regions III, IV, and V.

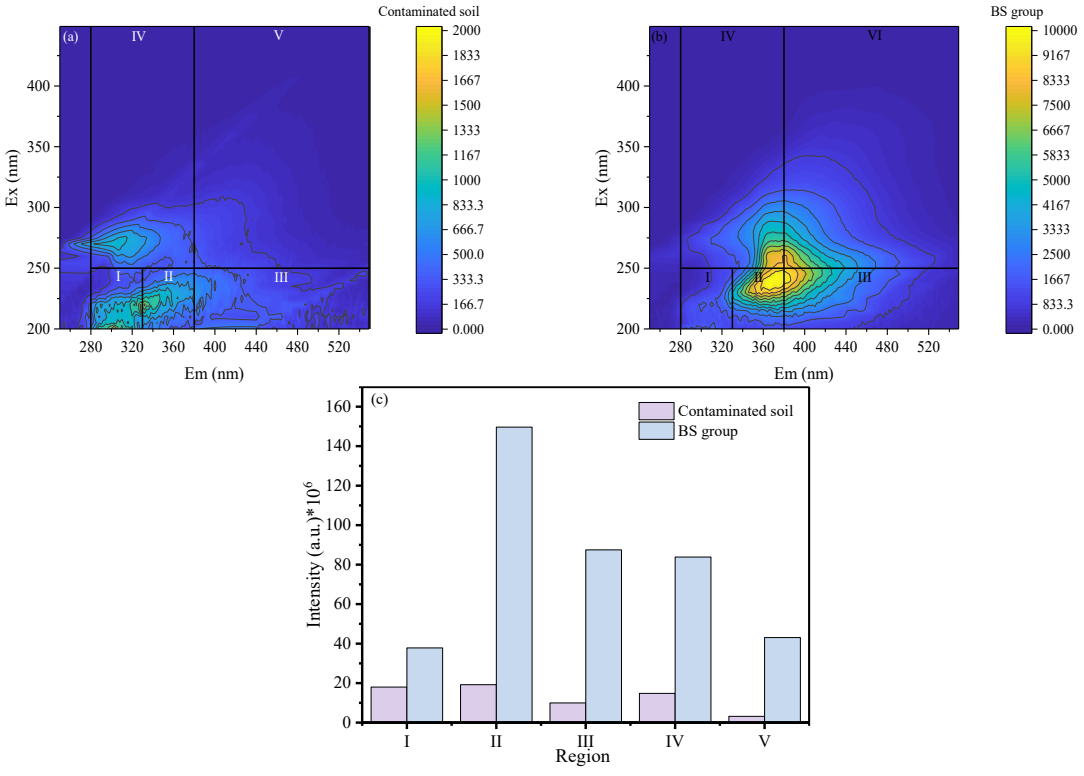

 doi:10.20944/preprints202602.1798.v1

Figure 4. Three-dimensional fluorescence excitation–emission matrix (3D-EEM) spectra (a-b) and integrated fluorescence volumes of each region (c) of contaminated soil and the BS group.

The integrated fluorescence volumes of each region are shown in Fig. 4c. For the original contaminated soil, the integrated volumes of regions I–V were 17986163.25, 19177989.8, 9974061.3, 14780727.44, and 3159094.84 au·nm², respectively. In contrast, the corresponding values in the BS group increased markedly to 37842111.38, 149662898.34, 87489665.46, 83846487.92, and 43058974.35 au·nm², respectively. The fluorescence intensities of humic-like and fulvic-like substances increased to 8.77 and 13.63 times those of the original contaminated soil, respectively. Overall, SPC^{SF} promoted the oxidation and fragmentation of petroleum hydrocarbons into bioavailable substrates, which supported microbial metabolism and facilitated the production of organic acids.

3.3.2. Microbial Stabilization of Fe(II) and Enhancement of Fenton Cycling

XPS analysis was conducted to further elucidate iron speciation. (SPC^{SF} combined with bacterial suspension). As shown in Fig. 5, the Fe 2p spectra of both the S group (SPC^{SF} alone) and the SB groups (SPC^{SF} combined with bacterial suspension) exhibited characteristic Fe 2p$_{3/2}$ and Fe 2p$_{1/2}$ peaks, along with associated satellite peaks arising from energy loss during photoemission. The Fe^{2+} 2p$_{3/2}$ and 2p$_{1/2}$ peaks were located at approximately 709.0 eV and 722.0 eV, whereas the corresponding Fe^{3+} peaks appeared near 711.0 eV and 724.0 eV.

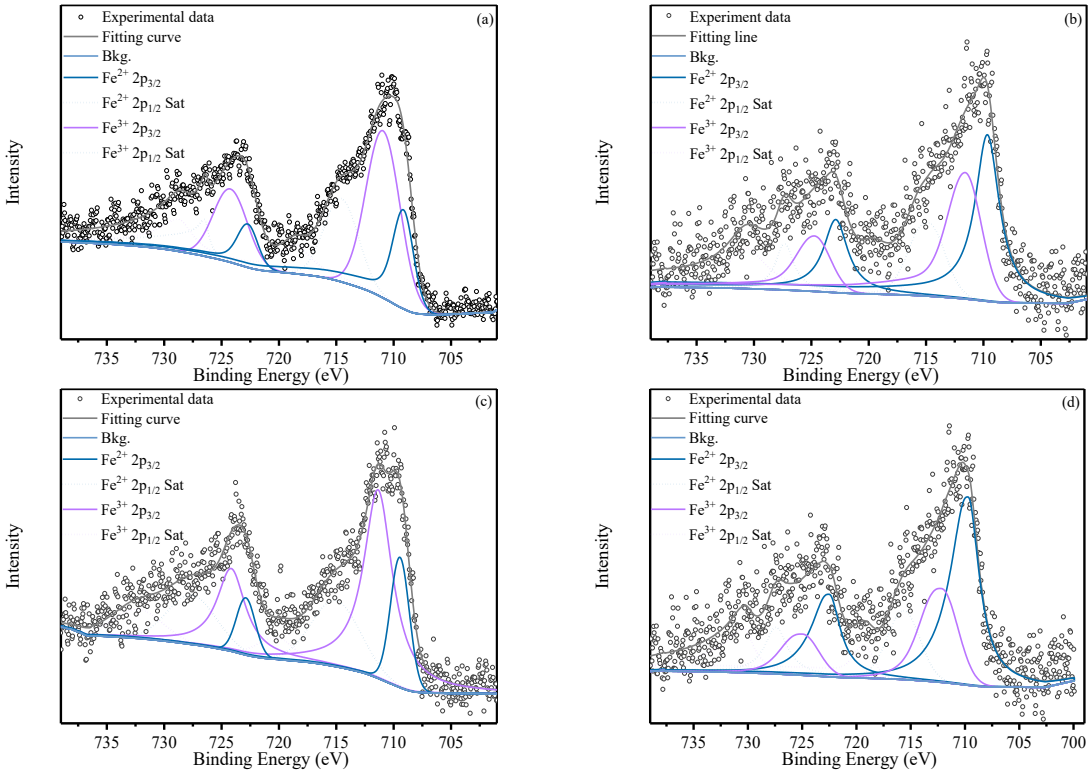

Figure 5. X-ray photoelectron spectroscopy (XPS) Fe 2p spectra of soil samples. (a) S1, (b) B30, (c) S1B30 and (d) S3B30.

In the S groups, the Fe 2p spectra were dominated by Fe^{3+} signals. Quantitative peak deconvolution yielded Fe^{2+}/Fe^{3+} ratios of 36.80%/63.20% in group S1 and 26.65%/73.35% in group S, indicating that iron predominantly existed in the Fe(III) state.

In contrast, the SB groups, particularly S1B30 and S3B30, exhibited substantially enhanced Fe^{2+} peak intensities. The Fe^{2+}/Fe^{3+} ratio increased to 53.38%/46.62% in S1B3 and further to 66.73%/33.27% in S3B3, corresponding to Fe^{2+} increases of 16.58% and 40.08% relative to S1 and S3, respectively. This consistent enrichment of Fe^{2+} highlights the critical role of *Bacillus subtilis* in promoting iron reduction and stabilization.

The Fenton reaction is governed by the cyclic redox transformation between Fe(II) and Fe(III), which sustains the continuous generation of hydroxyl radicals (·OH) for the oxidative degradation of

 doi:10.20944/preprints202602.1798.v1

petroleum hydrocarbons. Among the controlling factors, Fe(II) concentration is crucial for catalyzing hydrogen peroxide (H_2O_2) to produce ·OH. Therefore, microbial stabilization of Fe(II) directly enhances ·OH generation and accelerates contaminant degradation.

Moreover, because Fe(III) is prone to precipitation and deactivation under alkaline conditions, maintaining a high proportion of Fe(II) not only reduces total iron consumption but also supports the sustained and efficient operation of the Fenton reaction system. Based on the combined ORP and XPS results, *Bacillus subtilis* ATCC 11774 is inferred to enhance Fe(II) availability through enzymatic reduction processes.

3.3.3. Molecular-Scale Evidence for Carbon Structure Transformation

FTIR and XPS analyses were conducted to further elucidate carbon structure transformations at the molecular scale. The FTIR spectra of Groups S (SPC^{SF} only), SB (SPC^{SF} combined with bacteria), and B (bacteria only) are shown in Fig. 6. The absorption band at 3622 cm^{-1}, attributed to the hydration of clay minerals, exhibited significantly higher intensity in the microbial treatment groups (Groups B and SB) than in Group S. This enhancement reflects increased soil water-binding capacity associated with microbial activity.

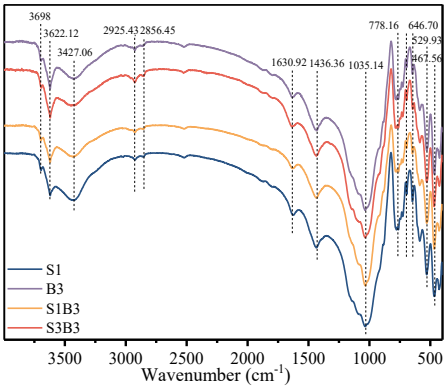

Figure 6. FTIR of soil samples. (a) S1, (b) B30, (c) S1B30 and (d) S3B30.

Characteristic absorption bands related to soil organic matter were observed at 2925 and 2856 cm^{-1}, corresponding to aliphatic C–H stretching vibrations, and at 1630 cm^{-1}, associated with –OH bending. Additional bands at 2960, 2896, 778, and 693 cm^{-1}, indicate the presence of residual aliphatic and aromatic hydrocarbon components.

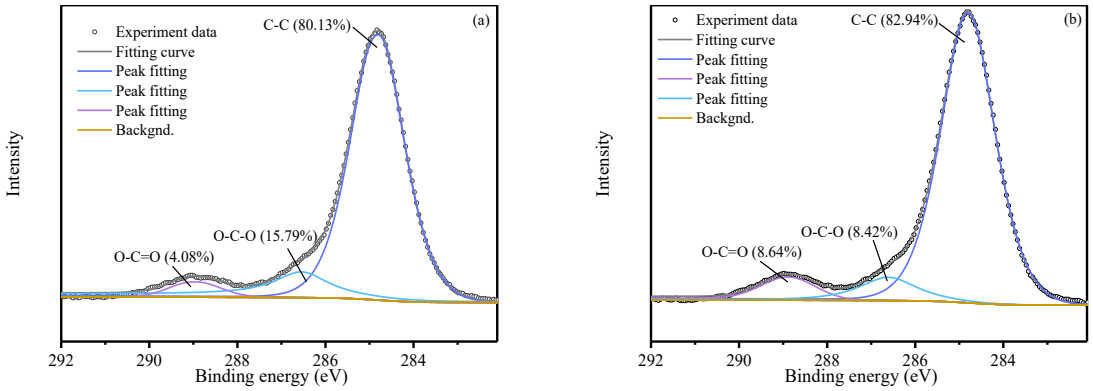

 doi:10.20944/preprints202602.1798.v1

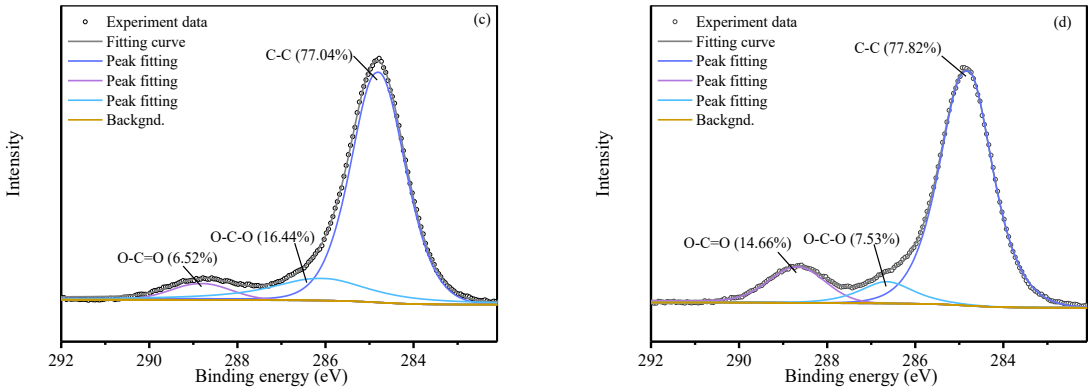

Figure 7. X-ray photoelectron spectroscopy (XPS) C 1s spectra of soil samples. (a) S1, (b) B30, (c) S1B30 and (d) S3B30.

Notably, the Si–O–Si stretching band at 1035 cm^{-1} was significantly more intense in Group SB than in Group S, suggesting enhanced removal of contaminants from clay mineral surfaces and increased exposure of kaolinite structural units. The absorption band at 1436 cm^{-1}, associated with carboxylic acid functional groups, also exhibited higher intensity in Group SB, indicating the formation of carboxyl-rich degradation intermediates driven by microbial activity.

XPS C 1s spectra (Fig. 7) further confirmed these transformations. Peaks at binding energies of 284.80 eV, 286.54 eV, and 288.95 eV were assigned to C–C, C–O–C, and O–C=O functional groups, respectively. At identical SPC^{SF} dosages, the relative intensity of the O–C=O peak was substantially higher in the SB groups than in the corresponding S groups (e.g., S1B3: 8.64% > S1: 4.08%; S3B3: 14.66% > S3: 6.52%), indicating enhanced conversion of oxidative intermediates into carboxylic acid metabolites.

Conversely, the relative intensity of C–O–C peak was markedly lower in the SB groups (S1B3: 8.42% > S1: 15.79%; S3B3: 7.53% > S3: 16.44%), suggesting active microbial utilization and transformation of epoxide intermediates ether- or epoxide-containing intermediates. Overall, the FTIR and XPS results demonstrate that microbial activity promotes the conversion of oxidized intermediates into more stable and mineralizable carboxyl-rich compounds, providing molecular-scale evidence for the enhanced degradation efficiency observed in the SB treatment.

4. Conclusions

This study developed a silica gel-loaded, iron-catalyzed sodium percarbonate composite (SPC^{SF}) and combined it with Bacillus subtilis ATCC 11774 for the remediation of diesel-contaminated soil. The simultaneous application of SPCSF and the bacterium achieved the highest removal efficiency (65.1% after 31 d), significantly outperforming chemical oxidation (22.5%) or microbial remediation alone (31.1%). The enhanced performance was attributed to a synergistic mechanism involving both chemical and biological processes.

SPC^{SF} played a dual role in the system: it generated reactive oxygen species for the oxidative breakdown of long-chain hydrocarbons into bioavailable intermediates, and it modulated soil physicochemical properties—particularly pH and oxidation-reduction potential—creating a more favorable environment for microbial activity. In turn, Bacillus subtilis facilitated the reduction and stabilization of Fe(II), sustaining the Fe(II)/Fe(III) redox cycle and thereby enhancing the generation of hydroxyl radicals in Fenton-like reactions.

Spectroscopic evidence from 3D-EEM, FTIR, and XPS revealed that the combined treatment promoted the transformation of petroleum hydrocarbons into carboxyl-rich organic matter, indicating effective mineralization and detoxification. The enrichment of Fe(II) and the conversion of ether-bonded intermediates into carboxylic acids provided molecular-scale confirmation of the synergistic interaction.

Overall, the SPC^{SF}–Bacillus subtilis system offers an efficient, environmentally compatible strategy for the remediation of petroleum hydrocarbon-contaminated soils. The findings provide mechanistic insights and support the potential field application of this combined approach. Future

 doi:10.20944/preprints202602.1798.v1

work should focus on optimizing delivery strategies, evaluating long-term ecological effects, and validating the system under real-world soil conditions.

Author Contributions: Conceptualization, Beibei Ren and Wei Wei; methodology, Wei Wei and Mingli Wei; investigation, Beibei Ren; resources, Siguang Zhao; data curation, Beibei Ren, Wei Wei, Mingli Wei, and Siguang Zhao; writing—original draft preparation, Siguang Zhao; writing—review and editing, Beibei Ren, Wei Wei, and Mingli Wei; supervision, Siguang Zhao; funding acquisition, Siguang Zhao. All authors have read and agreed to the published version of the manuscript.

Funding: This research was funded by the National Natural Science Foundation of China General Program, grant number 52478388; the Open Fund Project of Jiangsu Collaborative Innovation Center for Building Energy Saving and Construction Technology, grant number SJXTBS2113; the Industry–University–Research Collaborative Project of Jiangsu Province (2025), grant number BY20251569, and the Natural Science Foundation of Jiangsu Province (grant number BK20231153).

Data Availability Statement: Dataset available on request from the authors.

Conflicts of Interest: Author Mingli Wei was employed by the company Jiangsu Institute of Zoneco Co., Ltd. The re-maining authors declare that the research was conducted in the absence of any commercial or fi-nancial relationships that could be construed as potential conflicts of interest.

Abbreviations

The following abbreviations are used in this manuscript:

SPC	Sodium percarbonate
SPC^{SF}	A silica gel-loaded, iron-catalyzed SPC composite
ORP	Oxidation-reduction potential
LB	Luria-Bertani
OD_{600}	Optical density of the suspensions at a wavelength of 600 nm
DOM	dissolved organic matter
Ex	excitation wavelength
Em	emission wavelength
KBr	potassium bromide

References

1. Wei, W.; Wei, M.; Li, Y.; Xue, Q.; Liu, L.; Wan, Y., Macroscopic and molecular scale assessment of thermal effects on soil-water interactions of unsaturated diesel-contaminated soils. *Science of The Total Environment* **2024,** 951, 175695.
2. Wei, W.; Wei, M.; Li, Y.; Xue, Q.; Liu, L.; Wan, Y., Low-temperature treatment optimization for diesel-contaminated kaolin: Mutual impacts of generated pyrolytic carbon and particle agglomeration. *Environmental Pollution* **2024,** 363, 125196.
3. Gao, B.; Wang, X.; Ford, R. M., Chemotaxis along local chemical gradients enhanced bacteria dispersion and PAH bioavailability in a heterogenous porous medium. *Science of The Total Environment* **2023,** 859, 160004.
4. Xue, Y.; Chen, L.; Xiang, L.; Zhou, Y.; Wang, T., Experimental investigation on electromagnetic induction thermal desorption for remediation of petroleum hydrocarbons contaminated soil. *Journal of Environmental Management* **2023,** 328, 117200.
5. Mohanta, S.; Pradhan, B.; Behera, I. D., Impact and remediation of petroleum hydrocarbon pollutants on agricultural land: a review. *Geomicrobiology Journal* **2024,** 41, (4), 345-359.
6. Li, Y.-T.; Zhang, J.-J.; Li, Y.-H.; Chen, J.-L.; Du, W.-Y., Treatment of soil contaminated with petroleum hydrocarbons using activated persulfate oxidation, ultrasound, and heat: A kinetic and thermodynamic study. *Chemical Engineering Journal* **2022,** 428, 131336.
7. Majeed, B. K.; Shwan, D. M.; Rashid, K. A., A review on environmental contamination of petroleum hydrocarbons, its effects and remediation approaches. *Environmental Science: Processes & Impacts* **2025,** 27, (3), 526-548.

 doi:10.20944/preprints202602.1798.v1

8. Zhen, L.; Hu, T.; Lv, R.; Wu, Y.; Chang, F.; Jia, F. a.; Gu, J., Succession of microbial communities and synergetic effects during bioremediation of petroleum hydrocarbon-contaminated soil enhanced by chemical oxidation. *Journal of Hazardous Materials* **2021,** 410, 124869.
9. Mekonnen, B. A.; Aragaw, T. A.; Genet, M. B., Bioremediation of petroleum hydrocarbon contaminated soil: a review on principles, degradation mechanisms, and advancements. *Frontiers in Environmental Science* **2024,** 12, 1354422.
10. Kebede, G.; Tafese, T.; Abda, E. M.; Kamaraj, M.; Assefa, F., Factors influencing the bacterial bioremediation of hydrocarbon contaminants in the soil: mechanisms and impacts. *Journal of Chemistry* **2021,** 2021, (1), 9823362.
11. Ajoku, G.; Oduola, M., Kinetic model of pH effect on bioremediation of crude petroleum contaminated soil. 1. Model development. *American Journal of Chemical Engineering* **2013,** 1, (1), 6-10.
12. Zhang, B.; Guo, Y.; Huo, J.; Xie, H.; Xu, C.; Liang, S., Combining chemical oxidation and bioremediation for petroleum polluted soil remediation by BC-nZVI activated persulfate. *Chemical Engineering Journal* **2020,** 382, 123055.
13. Laurent, F.; Cébron, A.; Schwartz, C.; Leyval, C., Oxidation of a PAH polluted soil using modified Fenton reaction in unsaturated condition affects biological and physico-chemical properties. *Chemosphere* **2012,** 86, (6), 659-664.
14. Usman, M.; Jellali, S.; Anastopoulos, I.; Charabi, Y.; Hameed, B. H.; Hanna, K., Fenton oxidation for soil remediation: A critical review of observations in historically contaminated soils. *Journal of Hazardous Materials* **2022,** 424, 127670.
15. Kakosová, E.; Hrabák, P.; Černík, M.; Novotný, V.; Czinnerová, M.; Trögl, J.; Popelka, J.; Kuráň, P.; Zoubková, L.; Vrtoch, Ľ., Effect of various chemical oxidation agents on soil microbial communities. *Chemical Engineering Journal* **2017,** 314, 257-265.
16. Xu, Y.; Che, T.; Li, Y.; Fang, C.; Dai, Z.; Li, H.; Xu, L.; Hu, F., Remediation of polycyclic aromatic hydrocarbons by sulfate radical advanced oxidation: Evaluation of efficiency and ecological impact. *Ecotoxicology and Environmental Safety* **2021,** 223, 112594.
17. Zhang, L.; Jin, H.; Ma, H.; Gregory, K.; Qi, Z.; Wang, C.; Wu, W.; Cang, D.; Li, Z., Oxidative damage of antibiotic resistant E. coli and gene in a novel sulfidated micron zero-valent activated persulfate system. *Chemical Engineering Journal* **2020,** 381, 122787.
18. Gou, Y.; Ma, J.; Yang, S.; Song, Y., Insights into the effects of Fenton oxidation on PAH removal and indigenous bacteria in aged subsurface soil. *Environmental Pollution* **2022,** 298, 118872.
19. Sutton, N. B.; Langenhoff, A. A.; Lasso, D. H.; van der Zaan, B.; van Gaans, P.; Maphosa, F.; Smidt, H.; Grotenhuis, T.; Rijnaarts, H. H., Recovery of microbial diversity and activity during bioremediation following chemical oxidation of diesel contaminated soils. *Applied Microbiology and Biotechnology* **2014,** 98, (6), 2751-2764.
20. Molamahmood, H. V.; Qin, J.; Yu, S.; Long, M., Hydrogen peroxide decomposition into oxygen in different soils: Kinetic analysis, mechanism and implication in catalyzed hydrogen peroxide propagations. *Journal of Cleaner Production* **2021,** 304, 127116.
21. Meng, Q.; Wen, Z.; Sun, K.; Wang, Z.; Wang, M., Promotion of Chemical Oxidation of Polycyclic Aromatic Hydrocarbons in Soil by a Sodium Persulfate/Sodium Percarbonate Double-Oxidation System. *Chemistry & Biodiversity* **2025**, e01040.
22. Sheng, X.; Liu, Y.; Ali, M.; Habib, M.; Fu, R.; Lyu, S., Application of sulfidated nano zero-valent iron to enhance fluoranthene degradation by Fe (III) activated sodium percarbonate process in aqueous and soil media. *Journal of Environmental Chemical Engineering* **2024,** 12, (3), 113042.
23. Pan, H.; Yang, X.; Zhong, Y.; Xu, M.; Sun, G., Response of environmental variables and microbial community to sodium percarbonate addition to contaminated sediment. *Chemosphere* **2018,** 211, 500-509.